STRUCTURAL DESIGH AND MOTION ANALYSIS OF UNIVERSAL MOBILE QUADRUPED ROBOT

Wang Xiong
Yulin University
Shanxi, China
Email: 12296832@qq.com

Submitted: Mar. 30, 2016 ***Accepted: July 14, 2016*** ***Published: Sep. 1, 2016***

Abstract- According to bionics and simplified octopus structure, this paper designed a universal mobile quadruped robot and adopted Denavit-Hartenberg system to analyze the single leg kinematics of a robot, obtaining its kinematics equation. Also, through the method of separating variables, this paper solved its inverse kinematics and got the joint angle. A walking gait is planned and the joint angle of vertical pendulum stance phase and swing phase of the robot in walking are calculated. MATLAB is used to simulate the relevant joint angles of the robot, so as to analyze its movement change. Experimental results further verified the universal motion of robots.

Index terms*:* Universal motion, quadruped robot, kinematics, inverse kinematics, gait planning.

I. INTRODUCTION

In robot family, quadruped robots have become the study focus at home and abroad for its strong environmental adaptability and motion flexibility [1, 2, 3]. Most quadruped robots adopt bionics design, for example, Big Dog by Boston Propulsion Laboratory in the United States, which was designed according to the dog structure [4, 5]. However, in terms of the current development of quadruped robots and considering the simplification of control and structure in bionics design, domestic robot designers tend to simplify joints, which leads to unstable and inflexible motion of quadruped robots. Designers hope to design quadruped robots which can be simply controlled and stably and flexibly move with less degree of freedom [6, 7].

Based on bionic octopus structure, this paper designed a universal mobile quadruped robot and made motion analysis on it, aiming at making improvements in the above problems of quadruped robots.

II. STRUCTURE DESIGH OF UNIVERSAL MOBILE QUADRUPED ROBOT

Among land quadrupeds, most of them move in longitudinal direction while very few move in transverse direction. Among sea animals, octopus can move in multiple directions, shown as Figure 1.

The study on its structure found that it was due to the special placing of its joints. This study optimized its structure, changing 8 feet into 4 feet, shown as Figure 2. There are 16 degrees of freedom in total to inherit the placing of transverse and longitudinal joints of the octopus structure.

Figure 1. Octopus structure

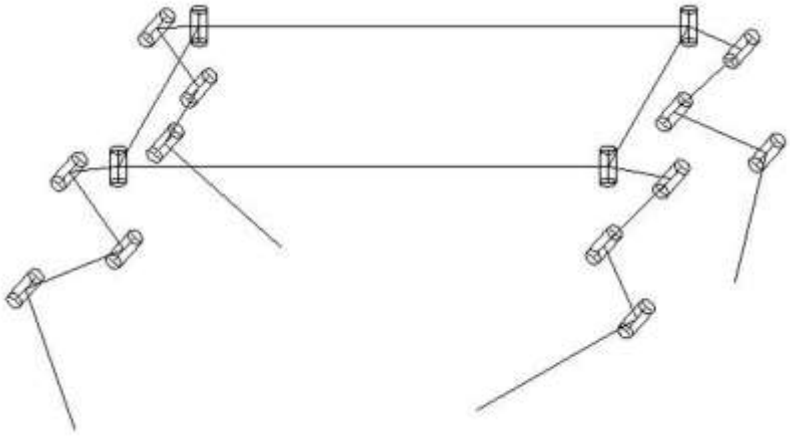

Figure 2. The electric power network with FCL in use

The simulation design was completed in software, shown as Figure 3. The real object is shown as Figure 4. The main body of universal mobile quadruped robots consists of controller, mounting base, transverse rotation motor, vertical rotation motor and mechanical structure components.

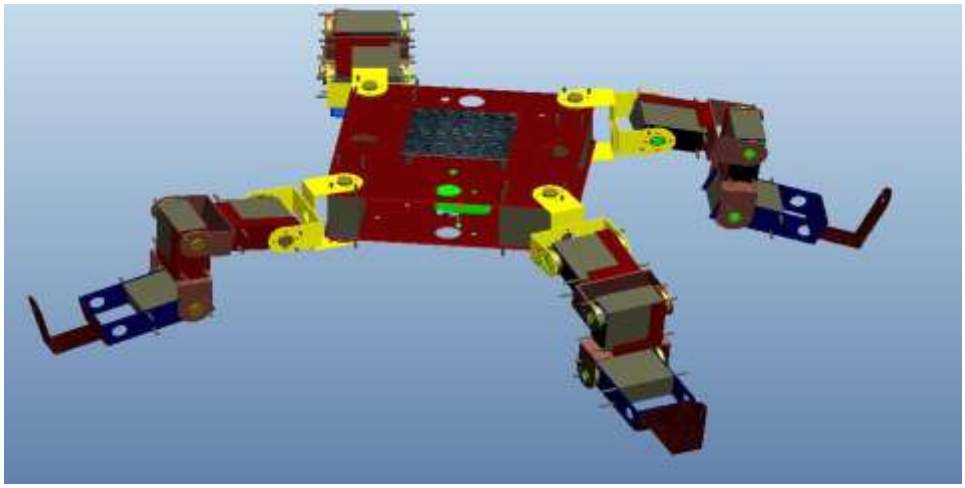

Figure 3. Simulation diagram of the structure of quadruped robots

4 transverse rotation motors and 4 vertical rotation motors are evenly distributed and fixed on the four angles of the mounting base, which are connected with the controller of the robot. The controller of the robot controls the transverse rotation according to the preset procedure, further realizing the motion of 4 feet in random direction in the transverse plane.

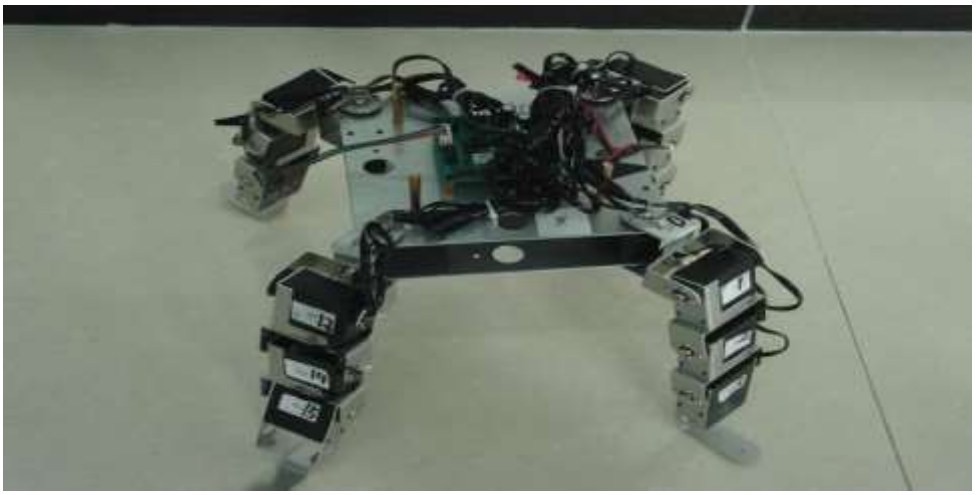

Figure 4. Simulation diagram of the structure of quadruped robots

Each transverse rotation motor is connected with 3 vertical rotation motors by mechanical structure component and the output axle centerline of the vertical rotation motor is perpendicular with that of transverse rotation motor in different planes. 12 vertical rotation motors are connected with the controller of the robot by wire. The controller of the robot controls the motion of 4 feet in random direction in the longitudinal plane according to the preset procedure.

The design of transverse and longitudinal joints realizes the universal motion of robots.

III. KINEMATICS EQUATION OF UNIVERSAL MOBILE QUADRUPED ROBOTS

To realize the universal motion of quadruped robots and better understand its kinematic performance, this paper made study on its kinematics.

a. Single leg modeling of robots and the determination of coordinate system

Four legs of universal mobile quadruped robot are the same. Thus, this paper studied one of them. Denavit-Hartenberg was utilized to establish the coordinate system and after the analysis and simplification [8, 9, 10, 11], the structure of a single leg is shown as Figure 5.

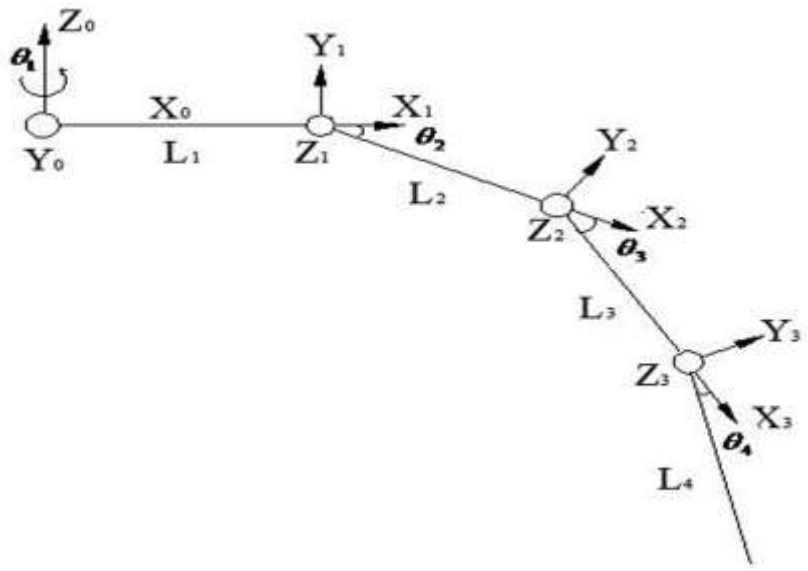

Figure 5. Coordinate system of the structure of a single leg.

Firstly the reference coordinate system is defined, namely, coordinate system {0}, which is fixed on the base, which is the main body of robot, namely, mounting plate (shown as Figure 4). According to relative motion, the definition is made. Here joint 1 is in transverse motion, with rotation angle of θ_1. The following coordinate systems {1}, {2} and {3} is of 90 degrees with {0} and the corresponding three joints, 2, 3 and 4 are in longitudinal motion, respectively with rotation angles of θ_2, θ_3 and θ_4. The coordinate system of each connecting rod is set at the joint. Y-axial of coordinate system {0} is perpendicular to the paper while Z-axial of other coordinate systems is perpendicular to the paper. X-axial is the extension cord of each connecting rod.

b. Determination of joint parameters and variables

i is the number of member bar, θ_i is joint variable, α_i is the torsion angle of the connecting rod, a_i is the length of the connecting rod, d_i is offset. The first joint axis is in vertical-state with other joint axes, so $\alpha_1 = 90°$. The left joint axes are parallel to each other. Thus,

$$\alpha_2 = \alpha_3 = \alpha_4 = 0° \qquad (1)$$

For simplification, the coordinate origin of each connecting rod is in the same plane. Thus,

$$d_1 = d_2 = d_3 = d_4 = 0 \qquad (2)$$

The parameters of A matrix (Denavit-Hartenberg Matrix) are shown as Table 1.

Table 1: Parameters of A matrix

i	θ_i	α_i	a_i	d_i	$\cos\alpha_i(c\alpha_i)$	$\sin\alpha_i(s\alpha_i)$
1	θ_1	90°	L_1	0	0	1
2	θ_2	0°	L_2	0	1	0
3	θ_3	0°	L_3	0	1	0
4	θ_4	0°	0	0	1	0

c. Solving of kinematics equation

A matrix is shown as Formula 3.

$$A_i = \begin{bmatrix} \cos\theta_i & -\sin\theta_i\cos\alpha_i & \sin\theta_i\sin\alpha_i & a_i\cos\theta_i \\ \sin\theta_i & \cos\theta_i\cos\alpha_i & -\cos\theta_i\sin\alpha_i & a_i\sin\theta_i \\ 0 & \sin\alpha_i & \cos\alpha_i & d_i \\ 0 & 0 & 0 & 1 \end{bmatrix} \tag{3}$$

Supposing, $c_i = \cos\theta_i$， $s_i = \sin\theta_i$， $i = 1$，2，3，4; $c_{ij} = \cos(\theta_i + \theta_j)$， $s_{ij} = \sin(\theta_i + \theta_j)$， $i = 1$，2，3，4； $j = 1$，2，3，4; $c_{ijk} = \cos(\theta_i + \theta_j + \theta_k)$， $s_{ijk} = \sin(\theta_i + \theta_j + \theta_k)$， $i = 1$，2，3，4； $j = 1$，2，3，4； $k = 1$，2，3，4.

Then, according to Table 1 and Formula 1, the homogeneous transformation matrix can be expressed as,

$$A_1 = \begin{bmatrix} c_1 & 0 & s_1 & L_1c_1 \\ s_1 & 0 & -c_1 & L_1s_1 \\ 0 & 1 & 0 & 0 \\ 0 & 0 & 0 & 1 \end{bmatrix} \tag{4}$$

$$A_2 = \begin{bmatrix} c_2 & -s_2 & 0 & L_2c_2 \\ s_2 & c_2 & 0 & L_2s_2 \\ 0 & 0 & 1 & 0 \\ 0 & 0 & 0 & 1 \end{bmatrix} \tag{5}$$

$$A_3 = \begin{bmatrix} c_3 & -s_3 & 0 & L_3c_3 \\ s_3 & c_3 & 0 & L_3s_3 \\ 0 & 0 & 1 & 0 \\ 0 & 0 & 0 & 1 \end{bmatrix} \quad (6)$$

$$A_4 = \begin{bmatrix} c_4 & -s_4 & 0 & 0 \\ s_4 & c_4 & 0 & 0 \\ 0 & 0 & 1 & 0 \\ 0 & 0 & 0 & 1 \end{bmatrix} \quad (7)$$

The attitude matrix of the reference coordinate system of the end connecting rod, T_4 is shown as Formula (8).

$$T_4 = A_1A_2A_3A_4 = \begin{bmatrix} c_1c_{234} & -c_1s_{234} & s_1 & c_1(L_1 + L_2c_2 + L_3c_{23}) \\ s_1c_{234} & -s_1s_{234} & c_1 & s_1(L_1 + L_2c_2 + L_3c_{23}) \\ s_{234} & c_{234} & 0 & L_2s_2 + L_3s_{23} \\ 0 & 0 & 0 & 1 \end{bmatrix} \quad (8)$$

IV. SOLVING OF INVERSE KINEMATICS OF UNIVERSAL MOBILE QUADRUPED ROBOT

The position matrix of robot end effector T, and key parameters are known, so joint variables can be solved, which provides preparations for the gait analysis of robots [12, 13, 14, 15].

The position matrix of end effector is shown as Formula (9).

$$T = T_4 = \begin{bmatrix} n_x & o_x & a_x & p_x \\ n_y & o_y & a_y & p_y \\ n_z & o_z & a_z & p_z \\ 0 & 0 & 0 & 1 \end{bmatrix} = \begin{bmatrix} c_1c_{234} & -c_1s_{234} & s_1 & c_1(L_1 + L_2c_2 + L_3c_{23}) \\ s_1c_{234} & -s_1s_{234} & c_1 & s_1(L_1 + L_2c_2 + L_3c_{23}) \\ s_{234} & c_{234} & 0 & L_2s_2 + L_3s_{23} \\ 0 & 0 & 0 & 1 \end{bmatrix} \quad (9)$$

Joint angle is solved by the method of separating variables, shown as Formula (10).

$$A_1^{-1}T_4 = A_2A_3A_4 = \begin{bmatrix} n_xc_1 + n_ys_1 & o_xc_1 + o_ys_1 & a_xc_1 + a_ys_1 & p_xc_1 + p_ys_1 - L_1 \\ n_z & o_z & a_z & p_z \\ n_xs_1 - n_yc_1 & o_xs_1 + o_yc_1 & a_xs_1 - a_yc_1 & p_xs_1 - p_yc_1 \\ 0 & 0 & 0 & 1 \end{bmatrix} \quad (10)$$

$$= \begin{bmatrix} c_{234} & -s_{234} & 0 & L_2c_2 + L_3c_{23} \\ s_{234} & c_{234} & 0 & L_2s_2 + L_3s_{23} \\ 0 & 0 & 1 & 0 \\ 0 & 0 & 0 & 1 \end{bmatrix}$$

a. Solving of θ_1

Take row 3 and line 4,

$$p_x s_1 - p_y c_1 = 0 \quad (11)$$

Then,

$$\theta_1 = \arctan\frac{p_y}{p_x} \quad (12)$$

$$\theta_1 = \theta_1 \pm 180° \quad (13)$$

When p_x and p_y are 0,

$$\theta_1 = 0 \quad (14)$$

The same is as below.

b. Solving of θ_3

Take row 3 and line 4 and row 4 and line 4. Then,

$$p_x c_1 + p_y s_1 - L_1 = L_2 c_2 + L_3 c_{23} \quad (15)$$

$$p_z = L_2 s_2 + L_3 s_{23} \quad (16)$$

θ_1 is known and take the squares of both sides of the equation. We can get,

$$c_3 = \frac{(p_x c_1 + p_y s_1 - L_1)^2 + p_z^2 - L_2^2 - L_3^2}{2L_2 L_3} \quad (17)$$

Its constraint condition is that the right side falls between -1 and 1.

$$s_3 = \pm\sqrt{1 - c_3^2} \quad (18)$$

Then,

$$\theta_3 = \arctan\frac{s_3}{c_3} \quad (19)$$

c. Solving of θ_2

Take row 3 and line 4 in Formula (9).

$$L_2 s_2 + L_3 s_{23} = p_z \quad (20)$$

θ_3 is known and after expansion, we can get,

$$c_2 L_3 s_3 + s_2(L_2 + L_3 c_3) = p_z \quad (21)$$

Then,

$$\theta_2 = \arctan\frac{L_2 + L_3 c_3}{L_3 s_3} \pm \arctan\frac{\sqrt{(L_3 s_3)^2 + (L_2 + L_3 c_3)^2 - {p_z}^2}}{p_z} \qquad (22)$$

d. Solving of θ_4

Take row 3 and line 1 and row 3 and line 2 in Formula (9).

$$\begin{cases} n_z = s_{234} \\ o_z = c_{234} \end{cases} \qquad (23)$$

then,

$$\theta_4 = \arctan\frac{n_z}{o_z} - \theta_2 - \theta_3 \qquad (24)$$

e. Solving of a case

Inverse kinematics was verified by a case. The end position and orientation is set as,

$$T = \begin{bmatrix} 0.612372 & -0.612372 & 0.5 & 143 \\ 0.353553 & -0.353553 & 0.866025 & 83 \\ 0.707107 & 0.707107 & 0 & 55 \\ 0 & 0 & 0 & 1 \end{bmatrix} \qquad (25)$$

The actual size of robot is L_1=L_2=L_3=L_4=60. According to the above algorithm, C programming language was used to write programs. After the unreasonable solutions are excluded, we can obtain the following solutions.

$$\theta_1 = 30.13^\circ, \theta_2 = 19.58^\circ, \theta_3 = 15.97^\circ, \theta_4 = 9.45^\circ$$

According to the above solutions, corresponding operations are made on robots to obtain the given end position and orientation, further proving the correction of the solution algorithm.

V. GAIT PLANNING AND VERIFICATION

Through the θ_1 to carry out the adjustment of the robot body and complete the body of universal deflection. In order to simplify the gait, θ_2 is to be a fixed angle. θ_3 and θ_4 are used to complete the gait planning.

a. Gait planning

A walking cycle of the robot is divided into two parts. In the first half of the cycle, the Left front and right back legs completes the vertical displacement of the body as the support phase in the

case of no movement of the foot tip. The right front and left back legs completes the forward movement of the swing phase.

In the second half of the cycle, The right front and left back legs completes the vertical displacement of the body as the support phase in the case of no movement of the foot tip. the Left front and right back legs completes the forward movement of the left foot tip as the swing phase[16,17,18,19].

Vertical pendulum completes the robot's walking. It is divided into the swing phase and support phase of vertical pendulum. Its movement changes in a cycle are shown in Table 2, in which Xline is the vertical step length. Take the left front foot as an example. In a cycle, when the left front foot swings vertically, the foot tip moves for 1/2Xline and the support phase of the right front leg also moves for 1/2Xline. Thus, its absolute movement is a step length.

Hip joint is used to measure the movement of the body. When the left front and right back legs swings vertically, the right front and left back legs support phase makes the hip joint move 1/2Xline. When being the support phase in another half of the cycle, it also moves 1/2XLine. In this way, the body moves for a step length absolutely.

Table2: Movement changes of the swing phase and support phase of vertical pendulum

Cycle	**0-1/4T**	**1/4T-1/2T**	**1/2T-3/4T**	**3/4T-T**
Support Phase	The hip joint on the left front and right back legs moves for 1/4XLine	The hip joint on the left front and right back legs moves 1/4XLine	The hip joint on the right front and left back legs moves for 1/4XLine	The hip joint on the right front and left back legs moves for 1/4XLine
Swing Phase	The foot tip of the right front and left back legs moves for 1/4XLine	The foot tip of the right front and left back legs moves for 1/4XLine	The foot tip of the left front and right back legs moves for 1/4XLine	The foot tip of the left front and right back legs moves for 1/4XLine

a.I Joint angle calculation of the swing phase of vertical pendulum

The analysis of the joint angle of the swing phase of vertical pendulum is shown in Figure 6. In the figure, H is the height from the axis of the hip joint to the ground and it is assumed to be constant in the walking cycle. In a cycle, the swing phase of each leg accounts for the half of the whole cycle (expressed by 0-0.5T in the paper). x and z are the movement values of the foot tips in the coordinate direction in the coordinate, respectively. The path amplitude of the foot tip to

the ground is Zline. The coordinate is shown in the figure, in which θ_3 and θ_4 are the calculation values of the hip joint angle and knee joint angle of the swing phase, respectively.

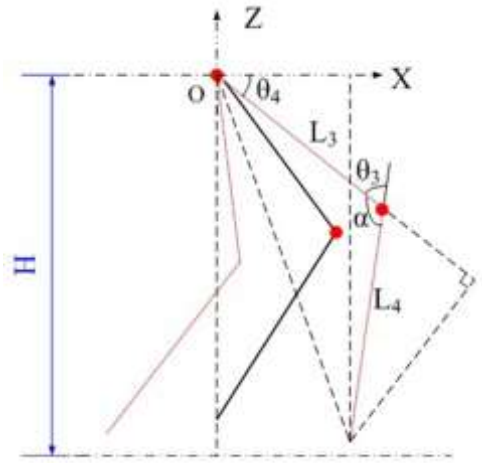

Figure 6. Joint angle of the swing phase of vertical pendulum

Since x direction is in the XOZ coordinate, relative to the origin O, it just moves for 1/2 Xline after completing swinging. The motion on x path is set to be uniform and the motion path of the foot tip along z direction is set to be the sinusoidal function, as shown in Formula (26).

$$\begin{cases} x = \dfrac{XLine}{T}t - \dfrac{1}{4}Xline & (0 \le t < 0.5T) \\ z = -H + Zline\sin(\pi t / 0.5T) & (0 \le t < 0.5T) \end{cases} \tag{26}$$

Given x and z, α can be calculated according to the Law of Cosines, as shown in Formula (27).

$$\alpha = a\cos(l_3^{\,2} + l_4^{\,2} - (x^2 + z^2)/(2l_3l_4)) \tag{27}$$

Thus, θ_3 and θ_4 are shown in Formula (28).

$$\begin{cases} \theta_3 = \pi - a\cos(l_3^{\,2} + l_4^{\,2} - (x^2 + z^2)/(2l_3l_4)) \\ \theta_4 = \pi - a\tan(|z/x|) - a\tan(l_4\sin\theta_2/(l_3 + l_4\cos\theta_2)) & (0 \le t < 0.25T) \\ \theta_4 = a\tan(|z/x|) - a\tan(l_4\sin\theta_2/(l_3 + l_4\cos\theta_2)) & (0.25T \le t < 0.5T) \end{cases} \tag{28}$$

a.II Joint angle calculation of the support phase of vertical pendulum

As shown in Figure 7, the ground support is within the support phase. That is, it does not move relative to the ground in 1/2 cycle. In the support phase, relative to the ground support, the axis of the hip joint moves for 1/2 of Xline. H is set to be constant. x and z are the movement values of

the foot tips in the coordinate direction in the coordinate system as shown in the figure, in which θ_3 and θ_4 are the calculation values of the hip joint angle and knee joint angle of the support phase, respectively.

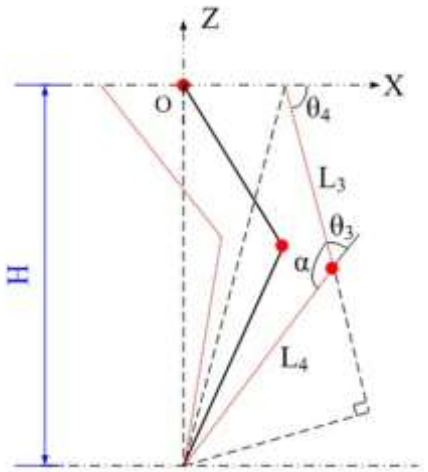

Figure 7. Joint angle calculation of the support phase

The support phase makes the uniform motion along the X axis in a half of cycle, as shown in Formula (29).

$$x = \frac{XLine}{T}t - \frac{1}{4}Xline \qquad (0 \le t < 0.5T) \qquad (29)$$

Thus, α can be obtained as shown in Formula(30).

$$\alpha = a\cos((l_3^{\,2} + l_4^{\,2} - (x^2 + z^2))/(2l_3l_4)) \qquad (30)$$

θ_3 and θ_4 are shown in Formula(31).

$$\begin{cases} \theta_3 = \pi - a\cos((l_3^{\,2} + l_4^{\,2} - (x^2 + z^2))/(2l_3l_4)) \\ \theta_4 = a\tan(|z/x|) - a\tan(l_4\sin\theta_2/(l_3 + l_4\cos\theta_2)) \quad (0 \le t < 0.25T) \\ \theta_4 = \pi - a\tan(|z/x|) - a\tan(l_4\sin\theta_2/(l_3 + l_4\cos\theta_2)) \quad (0.25 \le t < 0.5T) \end{cases} \qquad (31)$$

b. Simulation analysis

According to the actual size and expected gait of the robot, given YLine = 40, H = 160, XLine = 40, ZLine = 20.

The change of the vertical pendulum joint angle θ_3 is shown in Figure 8[16,17,18,19].

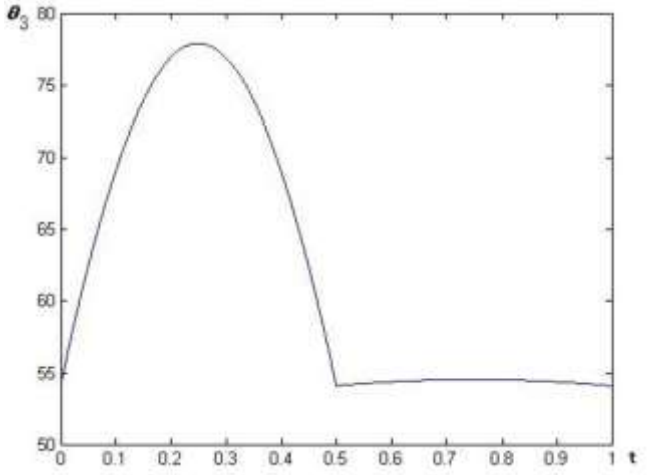

Figure 8. Vertical Pendulum Joint Angle θ_3

When the displacement in the vertical pendulum z direction is the sinusoidal curve, the change of its vertical pendulum joint angle θ_3 is the sinusoidal curve with the angle changing from 54.53°to 77.81°.The change in the second half of cycle is also the sinusoidal curve with the angle gently changing from 54.1°to 54.53°.

The change of the vertical pendulum joint angle θ_4 is shown in Figure 9.

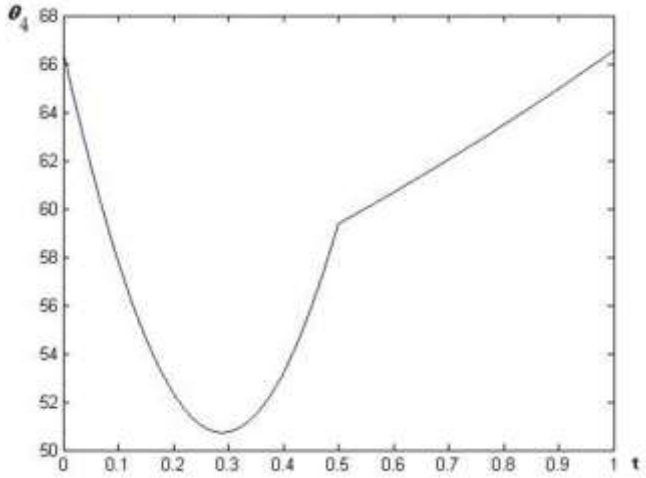

Figure 9. Vertical Pendulum Joint Angle θ_4

When the displacement in the vertical pendulum z direction is the sinusoidal curve, the change of

its vertical pendulum joint angle θ_4 is the sinusoidal curve in the first half of cycle with the angle changing from 51.05° to 66.53°. The change in the second half of cycle is nearly a sinusoidal curve with the angle gently changing from 59.38° to 66.53°.

c. Experimental verification

Motor and motor control panel are loaded and exterior decoration is made. According to the above algorithm and angle, solutions are got. After the procedure of angle gait is designed, the following universal mobile walking experiments can completed[20,21,22,23].

Shown as Figure 10, robot can move back and forth in longitudinal direction.

Figure 10. Movement back and forth direction

Shown as Figure 11, robot can move right and left in transverse direction.

Figure 11. Movement along right and left side

Shown as Figure 12, robot can move in slant of 40 degree without turning the engine body.

Figure 12. Movement at an angle of 40 degree

VI. CONCLUSIONS

This paper designed a quadruped robot according to bionic octopus structure and its legs were reasonably distributed in the engine body, enlarging the gravity domain of 4-feet robot, which increased the stability. At the same time, through experiment, it was verified that the robot can move in random direction without turning the engine body, which greatly enhanced its feasibility. The future study will focus on its kinetics analysis and intelligent control of sensors. This paper also can be reference to the studies of other kinds of robots.

VII. ACKNOWLEDGEMENTS

This work was financially supported by the university-industry cooperation projects of Yulin science and technology Bureau (2014cxy-08-02).

REFERENCES

[1] U.Saranli, M.Buehler, D.E.Koditschek, “A Simple and Highly Mobile Hexapod Robot”, Robotics Research, Vol. 20,No. 7, 2001, pp. 616-631.

[2] Keisuke Kato, Shigeo Hirose, “Development of Quardruped Walking Robot, TITAN-IX-Mechanical Design Concept and Application for the Humanitarian Demining Robot”, Advanced Robotics, Vol. 15, No. 2, 2001, pp. 191-204.

[3] Giannoccaro, Nicola Ivan, “ KINEMATIC TRAJECTORIES RECONSTRUCTION BASED ON MOTORS ENCODERS FEEDBACK FOR A ROVER SKID-STEERING ROBOT”, International Journal on Smart Sensing & Intelligent Systems, Vol. 8, No. 4, pp. 2116-2135, Dec 2015.

[4] Lianghong Ding, "Key technology analysis of BigDog quadruped robot", Chinese Journal of Mechanical Engineering, Vol. 51, No. 4, pp. 1-2, Apr 2015.

[5] Liang Yang, Song Xijia, Chunjian Deng, "OPPOSITION-BASED LEARNING PARTICLE SWARM OPTIMIZATION OF RUNNING GAIT FOR HUMANOID ROBOT", International Journal on Smart Sensing & Intelligent Systems, Vol. 8, No. 2, pp. 1162-1179, June 2015.

[6] Li Erchao, Li Zhanming , He Junxue, " ROBOTIC ADAPTIVE IMPEDANCE CONTROL BASED ON VISUAL GUIDANCE", International Journal on Smart Sensing & Intelligent Systems, Vol. 8, No. 4, pp. 2159-2174, Dec 2015.

[7] Hurmuzlu Y, Genot F, Brogliato B, “Modeling, stability and control of biped robots – A general framework”, Automatica, Vol. 40,No. 10, 2004, pp. 1647-1664.

[8] Hanazawa Y, Yamakita M., “Limit cycle running based on flat-footed passive dynamic walking with mechanical impedance at ankles”, Advanced Intelligent Mechatronics (AIM), 2012 IEEE/ASME International Conference on. IEEE, 2012: 15-20.

[9] Fu G P. “Research on Gait Planning and Walking Control for Humanoid Robot”, Guangdong University of technology, 2013.

[10] YE Changlong，MA Shugen，LI Bin, “Development of a shape-shifting mobile robot for urban search and rescue”, Chinese Journal of Mechanical Engineering, Vol. 21,No. 2, 2008, pp. 31-35.

[11] LI Zhiqing, MA Shugen,etal, "Development of a Transformable Wheel-track Robot with Self-adaptive Ability", China Mechanical Engineering, Vol. 47, No. 5, 2011, pp. 1-10.

[12] Li Junmin, Wang Jinge, Yang Simon X, Zhou Kedong, Tang Huijuan, "Gait Planning and Stability Control of a Quadruped Robot", Computational intelligence and neuroscience, Vol. 2016,, 2016, pp. 9853070.

[13] Baoping Wang, Renxi Hu, Xiaodong Zhang, Chuangfeng Huai, "Gait planning and intelligent control for a quadruped robot", Journal of Control Theory and Applications, Vol. 7, No. 2, 2009, pp. 207-211.

[14] Xianbao Chen, Feng Gao, Chenkun Qi, Xinghua Tian, "Gait planning for a quadruped robot with one faulty actuator", Chinese Journal of Mechanical Engineering, Vol. 28, No. 1, 2015, pp. 11-16.

[15] Brisswalter J, Fougeron B, Legros P, "Variability in energy cost and walking gait during race walking in competitive race walkers", Medicine and science in sports and exercise, Vol. 30, No. 9, 1998, pp. 1451-5.

[16] Ke Yang, Xu-yang Wang, Tong Ge, Chao Wu, "Simulation platform for the underwater snake-like robot swimming based on Kane's dynamic model and central pattern generator", Journal of Shanghai Jiaotong University (Science), Vol. 19, No. 3, 2014, pp. 294-301.

[17] Syed Atif Mehdi, Karsten Berns, Chao Wu, "Behavior-based search of human by an autonomous indoor mobile robot in simulation", Universal Access in the Information Society, Vol. 13, No. 1, 2014, pp. 45-58.

[18] Reynolds Raymond F, Bronstein Adolfo M, "Self-initiated gait increases susceptibility to the moving platform after-effect", NeuroReport, Vol. 17, No. 14, 2006, pp. 1503-5.

[19] Burke Conor S, McGaughey Orla, Sabattié Jean-Marc, Barry Henry, McEvoy Aisling K, McDonagh Colette, MacCraith Brian D, "Development of an integrated optic oxygen sensor using a novel, generic platform", The Analyst, Vol. 130, No. 1, 2004, pp. 41-5.

[20] Burke Conor S, McGaughey Orla, Sabattié Jean-Marc, Barry Henry, McEvoy Aisling K, McDonagh Colette, MacCraith Brian D, "Miniature robotic guidance for spine surgery--introduction of a novel system and analysis of challenges encountered during the clinical development phase at two spine centres", International Journal of Medical Robotics and Computer Assisted Surgery, Vol. 2, No. 2, 2007, pp. 146-53.

[21] Yamashita Yuichi, Tani Jun, "Emergence of functional hierarchy in a multiple timescale neural network model: a humanoid robot experiment", PL o S Computational Biology (Online), Vol. 4, No. 11, 2008, pp. e1000220.

[22] Tani Jun, Ito Masato, Sugita Yuuya, "Self-organization of distributedly represented multiple behavior schemata in a mirror system: reviews of robot experiments using RNNPB", Neural Networks, Vol. 17, No. 8-9, 2004, pp. 1273-89.

[23] Ampatzis Christos, Tuci Elio, Trianni Vito, Christensen Anders Lyhne, Dorigo Marco, Tani Jun, "Evolving self-assembly in autonomous homogeneous robots: experiments with two physical robots", Artificial Life, Vol. 15, No. 4, 2009, pp. 465-84.